Journal Pre-proofs

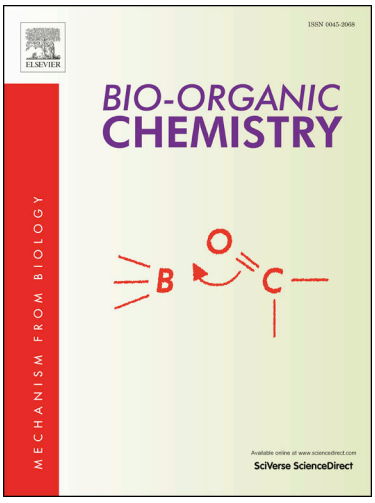

Synthesis and *in-vitro* anti-proliferative evaluation of some pyrazolo[1,5-*a*]pyrimidines as novel larotrectinib analogs

Mohamed H. Attia, Eman Z. Elrazaz, Soad Z. El-Emam, Azza T. Taher, Hatem A. Abdel-Aziz, Khaled A.M. Abouzid

PII: S0045-2068(19)31392-6
DOI: https://doi.org/10.1016/j.bioorg.2019.103458
Reference: YBIOO 103458

To appear in: *Bioorganic Chemistry*

Received Date: 26 August 2019
Revised Date: 12 November 2019
Accepted Date: 19 November 2019

Please cite this article as: M.H. Attia, E.Z. Elrazaz, S.Z. El-Emam, A.T. Taher, H.A. Abdel-Aziz, K.A.M. Abouzid, Synthesis and *in-vitro* anti-proliferative evaluation of some pyrazolo[1,5-*a*]pyrimidines as novel larotrectinib analogs, *Bioorganic Chemistry* (2019), doi: https://doi.org/10.1016/j.bioorg.2019.103458

Synthesis and *in-vitro* anti-proliferative evaluation of some pyrazolo[1,5-*a*]pyrimidines as novel larotrectinib analogs

Mohamed H. Attia[1], Eman Z. Elrazaz[2], Soad Z. El-Emam[3], Azza T. Taher[4], Hatem A. Abdel-Aziz[5*] and Khaled A.M. Abouzid[2,6*]

[1]*Department of Pharmaceutical Chemistry, Faculty of Pharmacy, October 6 University, 6 of October City, Giza, Egypt*

[2]*Pharmaceutical Chemistry Department, Faculty of Pharmacy, Ain Shams University, Abbassia 11566, Cairo, Egypt*

[3]*Department of Pharmacology and Toxicology, Faculty of Pharmacy, October 6 University, 6 of October City, Giza, Egypt*

[4]*Cairo University, Faculty of Pharmacy, Pharmaceutical Organic Chemistry Department, Cairo, Egypt*

[5]*Department of Applied Organic Chemistry, National Research Center, Dokki, Cairo 12622, Egypt*

[6]*Department of Organic and Medicinal Chemistry, Faculty of Pharmacy, University of Sadat City, Sadat City, Egypt*

ABSTRACT

A series of 2-phenyl-7-(aryl)pyrazolo[1,5-*a*]pyrimidine-3-carbonitriles **11a-j** and 2-phenyl-7-(aryl)pyrazolo[1,5-*a*]pyrimidine-3,6-dicarbonitriles **16a-c** was synthesized by the reaction of 5-amino-3-phenyl-1*H*-pyrazole-4-carbonitrile (**5**) with 3-(dimethylamino)-1-arylprop-2-en-1-ones **6a-j** or 2-aryl-3-(dimethylamino)acrylonitriles **12a-c**, respectively. In addition, 7-amino-5-oxo-2-phenyl-4,5-dihydropyrazolo[1,5-*a*]pyrimidine-3-carbonitrile (**22**) was prepared from the reaction of compound **5** with ethyl cyanoacetate. The anticancer activity of the newly synthesized compounds against Huh-7, HeLa, MCF-7 and MDA-MB231 cell lines showed moderate activity of compound **11f** as anti-proliferative agent against Huh-7 cell line with IC_{50} = 6.3 μM when compared with doxorubicin (IC_{50} = 3.2 μM). On the other hand, compound **16b** revealed potent anti-proliferative activity against HeLa cell line with IC_{50} = 7.8

μM when compared with doxorubicin (IC_{50} = 8.1 μM). Also compound **11i** exhibited a promising anti-proliferative activity against MCF-7 cell line (IC_{50} = 3.0 μM) whereas IC_{50} of doxorubicin = 5.9 μM, finally compounds **11i** and **16b** have potent activity as anti-proliferative agents against MDA-MB231 cell line with IC_{50} = 4.32 and 5.74 μM, respectively when compared with doxorubicin (IC_{50} = 6.0 μM).

Keywords: Synthesis, Pyrazolo[1,5-*a*]pyrimidine, Anticancer activity, MDA-MB231 cell line

*Corresponding authors: Khaled A.M. Abouzid, E-mail: khaled.abouzid@pharma.asu.edu.eg and Hatem A. Abdel-Aziz, E-mail: hatem_741@yahoo.com

1-Introduction

Pyrazolo[1,5-*a*]pyrimidine scaffold is an important block in the constructions of several anticancer agents [1-3]. For instance, the anticancer drug VITRAKVI® (Larotrectinib, **i**) (Fig 1), was innovated by medicinal scientists using pyrazolo[1,5-*a*]pyrimidine as core moiety [4]. VITRAKVI®, generated by Loxo Oncology Incorporation with Bayer and got FDA approval on November, 2018, is useful for treatments of solid tumors with gene fusion [5]. It showed potent anticancer activity as TRKA-C kinases inhibitor with IC_{50} < 1 nM and it revealed activity against TRKA G595R, TRKC G623R, and TRKA G667C cell lines with IC_{50} = 2.0-9.8 nM [6]. In addition, LOXO-195 (**ii**, Fig 1) is 2nd generation TRK inhibitor, it exhibited activity against TRK fusion- KM12, CUTO-3, and MO-91 cell line with IC_{50} ≤ 5 nM [6]. Furthermore, pyrazolo[1,5-*a*]pyrimidines **iii** (Fig 1) are useful for treatment of diseases associated with Interleukin-1 Receptor Associated Kinase (IRAK). These compounds modulate the function of IRAK-1 and/or IRAK-4 which represent an attractive approach to the development of therapeutic agents for the treatment of cancer, inflammatory and immune-related diseases [7].

On the other side, 3-(thiophene-2-carbonyl)pyrazolo[1,5-*a*]pyrimidine derivatives **iv** with aryl substitution in position 7 (Fig 1) showed potent activity as proliferative agents against HCT116 and 80S14 cell lines with IC_{50} = 11 and 0.45 μM respectively [8] and they revealed a significant anticancer activity against different six colon cell lines with IC_{50} = 0.012-2.3 μM [9].

pyrazolo[1,5-*a*]pyrimidines **v** (Fig 1), with phenyl moiety in position 2, have been reported as CDK inhibitors. Their anticancer activity against A549, DU-145, ACHN, MCF-7 and Hela cell lines with IC_{50} in the range of 1.94-7.07 µM [10].

Pyrazolo[1,5-*a*]pyrimidine **vi** (Fig 1), with carbonitrile function in position 3, has been reported as potent anticancer agents against Bel-7402 and HT-1080 cell lines [11], whereas pyrazolo[1,5-a]pyrimidine-3-carbonitrile **vii** (Fig 1) showed potent anticancer activity (IC_{50} = 0.002 µM) against HCT116 cell line [12]. Furthermore, 7-amino-pyrazolo[1,5-*a*]pyrimidines **viii** and **ix** (Fig 1) have been reported as potent Lck and CHK1 inhibitors, respectively [13][14].

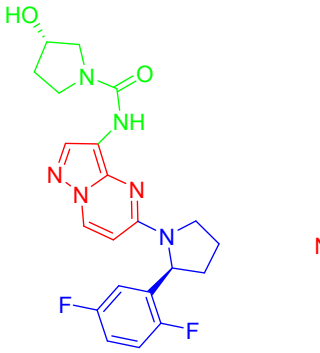

i, VITRAKVI® (Larotrectinib)

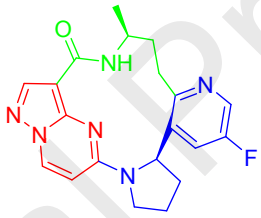

ii, LOXO-195

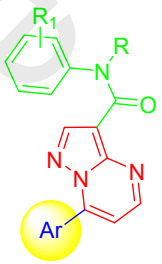

iii

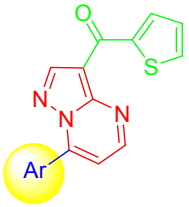

iv

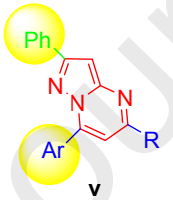

v

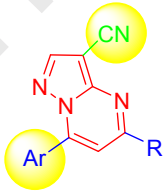

vi

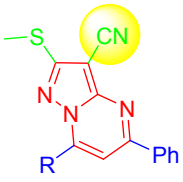

vii

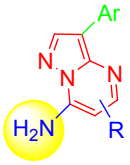

viii, Ar = 3-substituted phenyl
ix, Ar = substituted pyrazol-3-yl

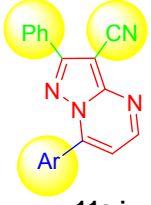

11a-j

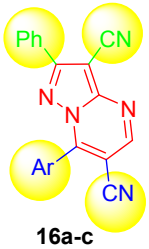

16a-c

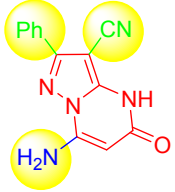

22

Figure 1. Structure of **i** (Larotrectinib), **ii** (LOXO-195), **iii-ix** and the target compounds **11a-j**, **16a-c**, and **22**.

In view of the previous reports [4-15], we aim to report herein the synthesis of 7-aryl-2-phenylpyrazolo[1,5-*a*]pyrimidine-3-carbonitriles **11a-j**, 7-aryl-2-phenylpyrazolo[1,5-*a*]pyrimidine-3,6-dicarbonitriles **16a-c** and 7-amino-2-phenylpyrazolo[1,5-*a*]pyrimidine-3-carbonitrile **22** as larotrectinib analogs to evaluation their anticancer properties against four human cancer cell lines namely; Huh-7, HeLa, MCF-7 and MDA-MB231 cell lines.

2-Results and Discussion

2.1. Chemistry

The key starting material 5-amino-3-phenyl-1*H*-pyrazole-4-carbonitrile (**3**) was prepared by the reaction of 3-oxo-3-phenylpropanenitrile (**1**) with trichloroacetonitrile to yield 3-amino-2-benzoyl-4,4,4-trichlorobut-2-enenitrile (**2**) which then reacted with hydrazine hydrate (Scheme 1). There are two alternative methods have been reported for the synthesis of **3** by reacting arylmethylenemalononitrile with hydrazine [16-17] or *via* transformation of isoxazoles using hydrazine [18]. On the other hand, enaminones 3-(dimethylamino)-1-arylprop-2-en-1-ones **6a-j** are versatile substrates in the synthesis of several biologically active heterocyclic compounds and drug intermediates, were chosen in this study for the synthesis of pyrazolo[1,5-*a*]pyrimidines **11a-j**. Enaminones **6a-j** are generally prepared by the condensation of methyl aryl ketones **4a-j** with dimethylformamide dimethylacetal (**5**) in refluxing xylene (Scheme 1) [19-22]. Next, the reaction of 5-amino-3-phenyl-1*H*-pyrazole-4-carbonitrile (**3**) with enaminones **6a-j** in refluxing acetic acid resulted in the formation of 2-phenyl-7-(aryl)pyrazolo[1,5-*a*]pyrimidine-3-carbonitriles **11a-j**, respectively**.** The latter reaction was assumed to proceed through an initial *Michael* type addition of the amino group in pyrazole **3** to the double bond in enaminones **6a-j** to give intermediate **7a-j** followed by the elimination of dimethylamine to afford the non-isolable intermediates **8a-j** which cyclized by losing one mole of H_2O to give pyrazolo[1,5-*a*]pyrimidines **11a-j** as final isolable products (Scheme 1). The ^{1}H NMR spectra of **11a-j** showed the down-field doublet signal of pyrimidine H2 at δ 8.78–8.96 with J = 4.4–6.0 Hz, whereas the up-field doublet signal of pyrimidine H3 appeared at δ around 7.61 with J around 5.8 Hz whereas the signal of amino group not appeared in their NMR spectra. In addition, the mass spectra of **11a-j** exhibited, in each case, a peak corresponding to their molecular ions. The IR spectra of **11a-j**

revealed the absence of the characteristic absorption band in the region 3150-3400 cm^{-1} due to amino group.

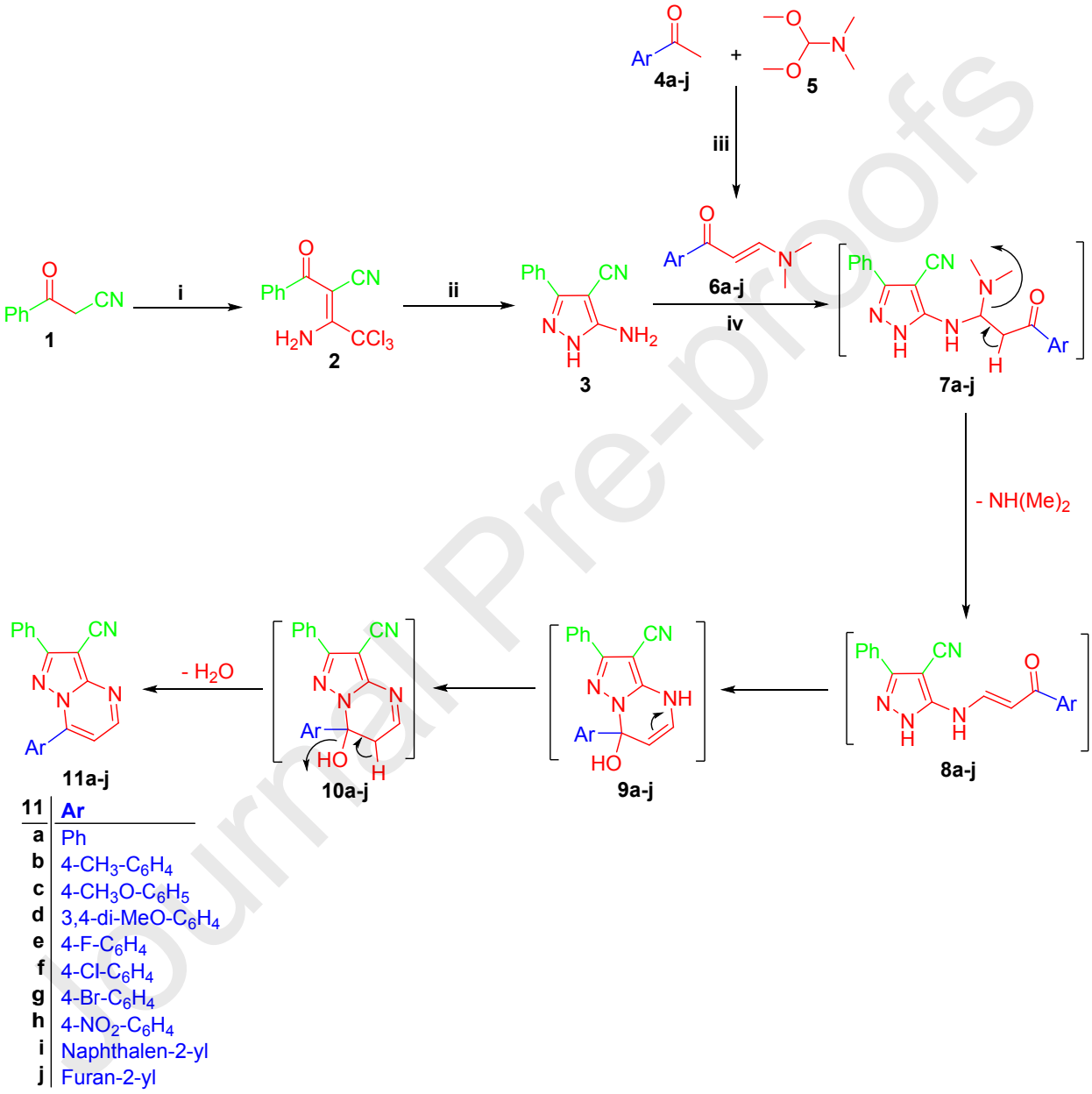

11	Ar
a	Ph
b	4-CH_3-C_6H_4
c	4-CH_3O-C_6H_5
d	3,4-di-MeO-C_6H_4
e	4-F-C_6H_4
f	4-Cl-C_6H_4
g	4-Br-C_6H_4
h	4-NO_2-C_6H_4
i	Naphthalen-2-yl
j	Furan-2-yl

Scheme 1. **Reagents and conditions**: **i**) Cl_3C-CN/anhydrous CH_3COONa/abs. EtOH/stirring 48 h; **ii**) NH_2-NH_2.H_2O/abs. EtOH/reflux 4 h; **iii**) dry xylene/reflux 8h; **iv**) glacial AcOH/reflux 3 h.

Furthermore, the reaction of pyrazole **3** with 2-aryl-3-(dimethylamino)acrylonitrile **12a-c** in refluxing acetic acid resulted in the formation of the corresponding pyrazolopyrimidines **16a-c**. Their ^{1}H NMR spectra revealed the down-field singlet signal of H2 proton of pyrimidine moiety in the region δ 9.04–9.25 and the signal of amino group not appeared in their NMR spectra, whereas their mass spectra showed a peak corresponding to their molecular ion values. The IR spectra of **16a-c** revealed the characteristic sharp absorption band of two carbonitrile groups in the region 2230-2240 cm^{-1} and the absence of amino group absorption band in the region 3150-3400 cm^{-1}. This reaction was proposed to proceed through the same reaction pathway of compounds **16a-c** (Scheme 1). However, the possible structure **18a-c** is easily excluded on the basis of the spectral data of the isolated products (Scheme 2).

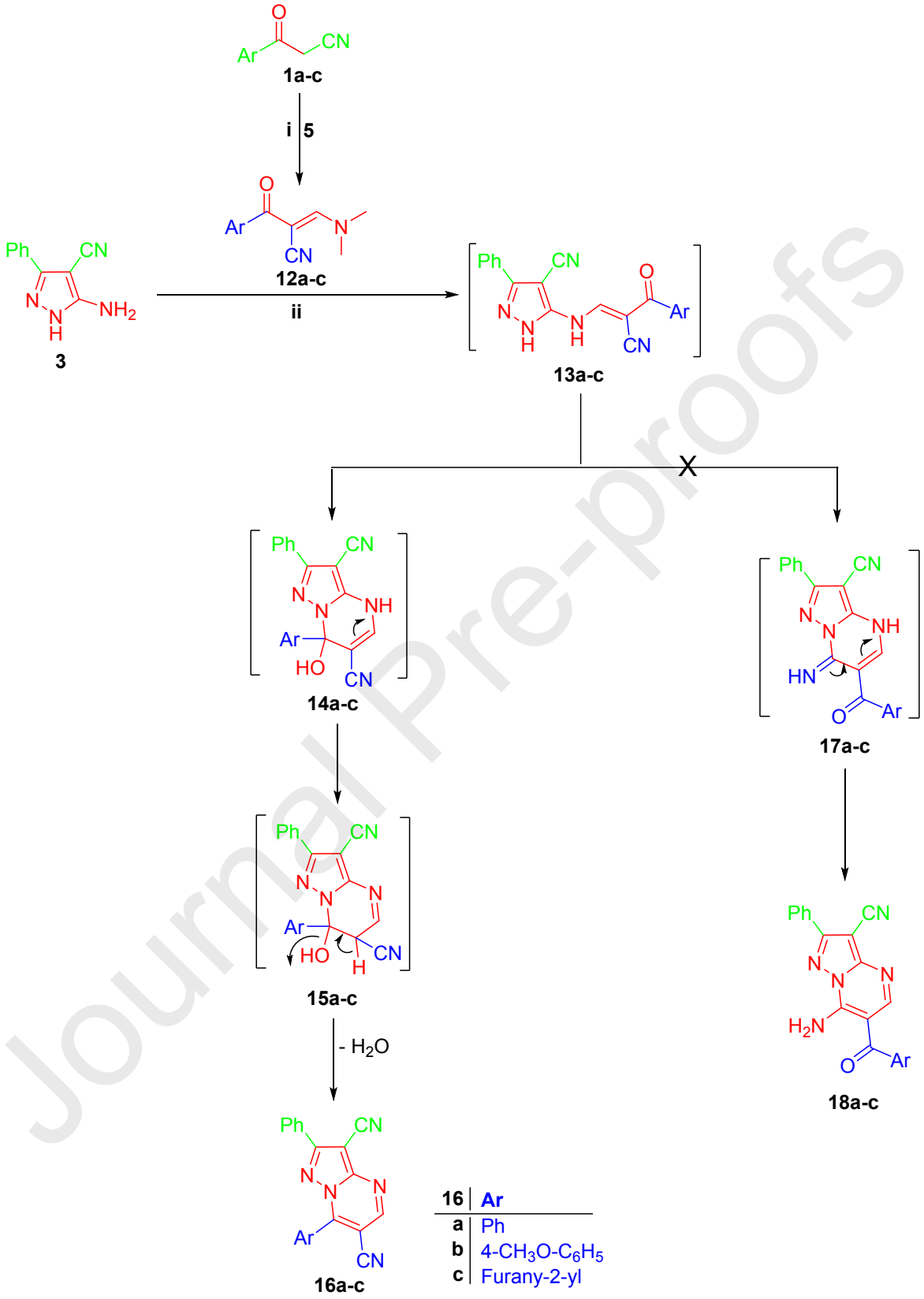

Scheme 2. **Reagents and conditions**: **i**) dry xylene/reflux 1 h; **ii**) glacial AcOH/reflux 3 h.

Next, the neat reaction of compound **3** with ethyl cyanoacetate (**19**) gave 7-amino-5-oxo-2-phenyl-4,5-dihydropyrazolo[1,5-*a*]pyrimidine-3-carbonitrile (**22**) (Scheme 3). The IR spectrum of **22** showed absorption band due to the carbonyl group at 1685 cm^{-1}. ^1H NMR spectrum of **22** revealed two D_2O exchangeable signals at δ 7.77 and 12.07 which were assigned to NH_2 and NH protons, respectively. Furthermore, the acetylation of compound **3** with glacial acetic acid gave *N*-(4-cyano-3-phenyl-1*H*-pyrazol-5-yl)acetamide (**23**). The IR spectrum of **23** showed a carbonyl band at 1685 cm^{-1}. ^1H NMR spectrum of **23** revealed two D_2O exchangeable signals at δ 10.73 and 13.67 which were assigned to NH of $COCH_3$ and NH of pyrazole protons, respectively. Finally, diazotization of compound **3** yielded the corresponding diazonium chloride **24** which was coupled with 3-oxo-3-phenylpropanenitrile (**1**) to give the corresponding hydrazone **25** (Scheme 3). The IR spectrum of **25** showed a carbonyl absorption band at 1650 cm^{-1}. ^1H NMR spectrum of **25** revealed two D_2O exchangeable signals at δ 9.61 and 9.91 which were assigned to the protons of hydrazone NH and pyrazole NH, respectively.

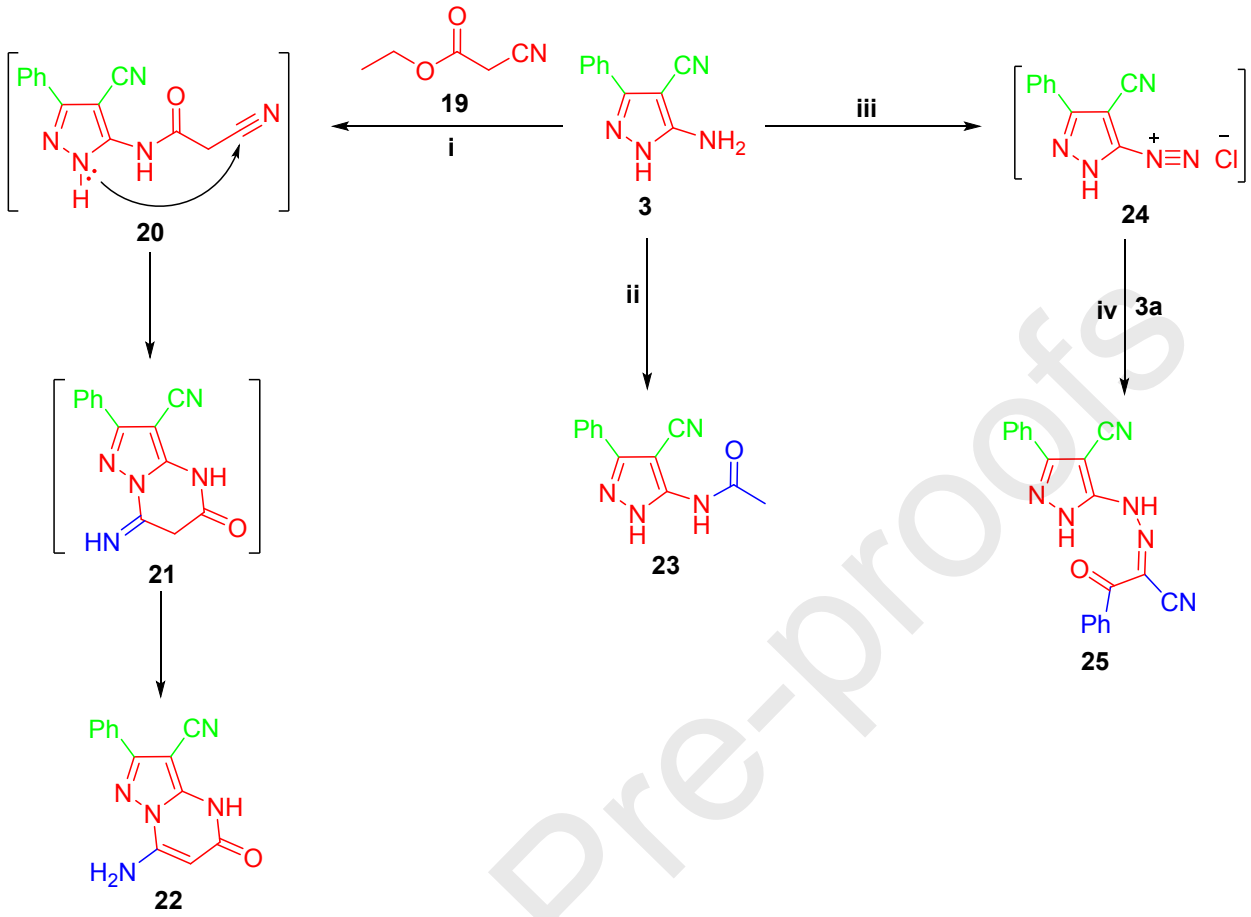

Scheme 3. **Reagents and conditions**: **i**) fusion, 45 min; **ii**) AcOH/reflux 2 h; **iii**) AcOH/HCl/$NaNO_2$/0-5°C; **iv**) $CH_3COONa.3H_2O$/abs. EtOH/stirring 4 h, 0-5°C.

2.2. Anticancer Activity

2.2.1. *In vitro* anti-proliferative activity against Huh-7, HeLa and MCF-7 cell lines

All synthesized pyrazolo[1,5-*a*]pyrimidines **11a-j**, **16a-c**, **22** in addition to *N*-(4-cyano-3-phenyl-1*H*-pyrazol-5-yl)acetamide **23** and *N*-(4-cyano-3-phenyl-1*H*-pyrazol-5-yl)-2-oxo-2-phenylacetohydrazonoyl cyanide **25** were examined for their antiproliferative activity towards three cancer cell lines: hepatocellular carcinoma Huh-7, cervical adenocarcinoma HeLa and breast adenocarcinoma MCF-7 cell lines. The MTT colorimetric assay was adopted to assess the anti-proliferative activity as described by Mosmann [23]. Doxorubicin was used as a control in this assay. The results were expressed as median growth inhibitory concentration (IC_{50}) values that represent the compound concentration required to produce a 50% inhibition of cell growth after 24 h of incubation (Table 1). The results of the MTT assay listed in Table 1 suggested that

the examined compounds **11a-j**, **16a-c**, **22**, **23** and **25** exhibited growth inhibitory activity against the tested Huh-7, HeLa and MCF-7 cancer cell lines. Huh-7 and HeLa cells were found to be more sensitive to the impact of the tested compounds than MCF-7 cells, except compound **11i** which is more effective towards MCF-7 cells. Compounds **11f**, **16b** and **11i** emerged as the most active compounds towards Huh-7, HeLa and MCF-7 cell lines with IC_{50} values equal 6.3, 7.8 and 3.0 μM, respectively, which are comparable to those of Doxorubicin (IC_{50} = 3.2, 8.1 and 5.9 μM, respectively). Regarding the activity of tested compounds against Huh-7 cells, compounds **16a** and **23** displayed moderate antitumor activity with IC_{50} values in the range of 10.2–29.1 μM, whereas the compounds **16b** and **25** exhibited a significant potency towards Huh-7 cell line with IC_{50} values 53.7 and 54.1 μM, respectively. On the other hand, investigation of the anti-proliferative activity against HeLa cell line elucidated that **11c**, **11i**, **16a** and **16c** had moderate anti-proliferative activity with IC_{50} values equal 25.3, 21.6, 15.5 and 26.2 μM, respectively. Furthermore, compounds **11d**, **11e**, **11f**, **11h**, **11j**, **22**, **23** and **25** were significantly active towards Huh-7 cells with IC_{50} values of 56.4, 39.6, 48.8, 60.2, 55.6, 62.6, 44.6 and 56.6 μM, respectively. Finally, the anti-proliferative activity against MCF-7 cell line elucidated that **11a** and **11e** were significantly active towards MCF-7 cells with IC_{50} values of 39.3 and 49.0 μM, respectively.

Table 1. *In vitro* anti-proliferative activity of the synthesized compounds against Huh-7, HeLa and MCF-7 cell lines

Compound	IC_{50} (μM)		
	Huh-7	**HeLa**	**MCF-7**
11a	77.5	245.2	39.3
11b	109.5	155.1	507.4
11c	123.6	25.3	194.9
11d	75.2	56.4	171.4
11e	75.2	39.6	49.0
11f	6.3	48.8	118.4
11g	88.4	79.1	84.2
11h	70.9	60.2	87.8
11i	95.0	21.6	3.0
11j	82.6	55.6	100.5
16a	29.1	15.5	133.8
16b	54.1	7.8	106
16c	65.6	26.2	70.1
22	83.1	62.6	189.3
23	10.2	44.6	247.0
25	53.7	56.6	71.2
DOX	3.2	8.1	5.9

2.2.2. In vitro anti-proliferative activity of 11f, 11i and 16b against MDA-MB231 cell lines

The promising results of compounds **11f**, **11i** and **16b** against the tested cell lines stimulate our interest to evaluate their antiproliferative potency against the MDA-MB231 cell lines. Interestingly, compounds **11i** and **16b** showed potent antiproliferative activity with IC_{50} 4.32 μM and 5.74 μM, respectively, when compared with that of Doxorubicin with IC_{50} = 6 μM (Table 2).

Table 2. *In vitro* anti-proliferative activity of compounds **11f**, **11i** and **16b** against MDA-MB231 cell lines.

Compound	IC_{50} (μM)
11f	74.25
11i	4.32
16b	5.74
DOX	6.0

2.2.3. Structure activity relationship (SAR)

Observing the results, we could deduce valuable data about the structure activity relationship (SAR). Firstly, Huh-7 cell line on investigation of the impact of the substitution on the pendant phenyl group in compounds **11a** revealed that grafting a chloro group (**11f**, IC_{50} = 6.3 μM) is more beneficial for activity than fluoro and bromo group (**11e**, IC_{50} = 75.2 μM and **11g**, IC_{50} = 88.4 μM, respectively) independent on the electronic displacement effect of Cl atom. The effect of replacement of pyrimidine ring in pyrazolopyrimidine **11f** (IC_{50} = 6.3 μ M) with *N*-acetyl group in compound **23** (IC_{50} = 10.2 μM), resulted in remarkable decrease in the activity. Also, introduce of cyano group in position 4 of pyrimdine ring in compounds **11a** and **11c** (IC_{50} = 77.5 and 25.3 μM, respectively) resulted in an increase of the anti-proliferative activity of compounds **16a** and **16b** (IC_{50} = 29.1 and 6.8 μM, respectively) against Huh-7 and HeLa cell lines respectively. In HeLa cell lines, the substitution on the pendant phenyl group with methoxy function in compound **16b** (IC_{50} = 6.8 μM) is more beneficial for activity than unsubstituted phenyl group in compound **16a** (IC_{50} 15.5 = μM). In MCF-7 cell lines, the effect of replacement of phenyl ring in compound **11a** (IC_{50} = 39.3 μM) with more lipophilic naphthalene group increase the activity in compound **11i**, (IC_{50} = 3.0 μM) resulted in remarkable increase in the activity. In MDA-MB231 cell lines, compound **11i** with lipophilic naphthyl substitution and compound **16b** with 4-methoxyphenyl substitution showed potent antiproliferative activity (IC_{50} = 4.32 and 5.74 μM, respectively) whereas compound **11f** with 4-chlorophenyl substitution showed very low antiproliferative activity (IC_{50} = 74.25 μM) when compared with **11f** or **16b**.

2.2.4. Effect of compound 11f, 11i and 16b on cell cycle distribution of Huh-7, HeLa, MCF-7 and MDA-MB231 cell lines after 48 h incubation

The ability of compounds **11f**, **11i** and **16b** to induce cell cycle growth arrest was assessed by using the PI/RNase staining solution for quantification of DNA content under each phase of the cell cycle and subsequent analysis by flow cytometry. As shown in Figure 2, treatment of MCF-7 cells with compound **11i** for 48 h induced a marked reduction in G1 phase, with significant arrest in S phase as well as G2/M phase when compared to that of control untreated cells ($P < 0.05$). In Figure 3, treatment of MDA-MB-231 cells with compound **11i** for 48 h induced a significant arrest in G1 phase, with marked reduction in S phase when compared to that of control untreated cells ($P < 0.05$). Also, treatment of Hela cells with compound **16b** for 48 h induced a marked reduction

in G1 phase, with significant arrest in G2/M phase when compared to that of control untreated cells (Fig 4). Finally, treatment of Huh-7 cells with compound **11f** for 48 h showed no change when compared with that of control untreated cells ($P < 0.05$).

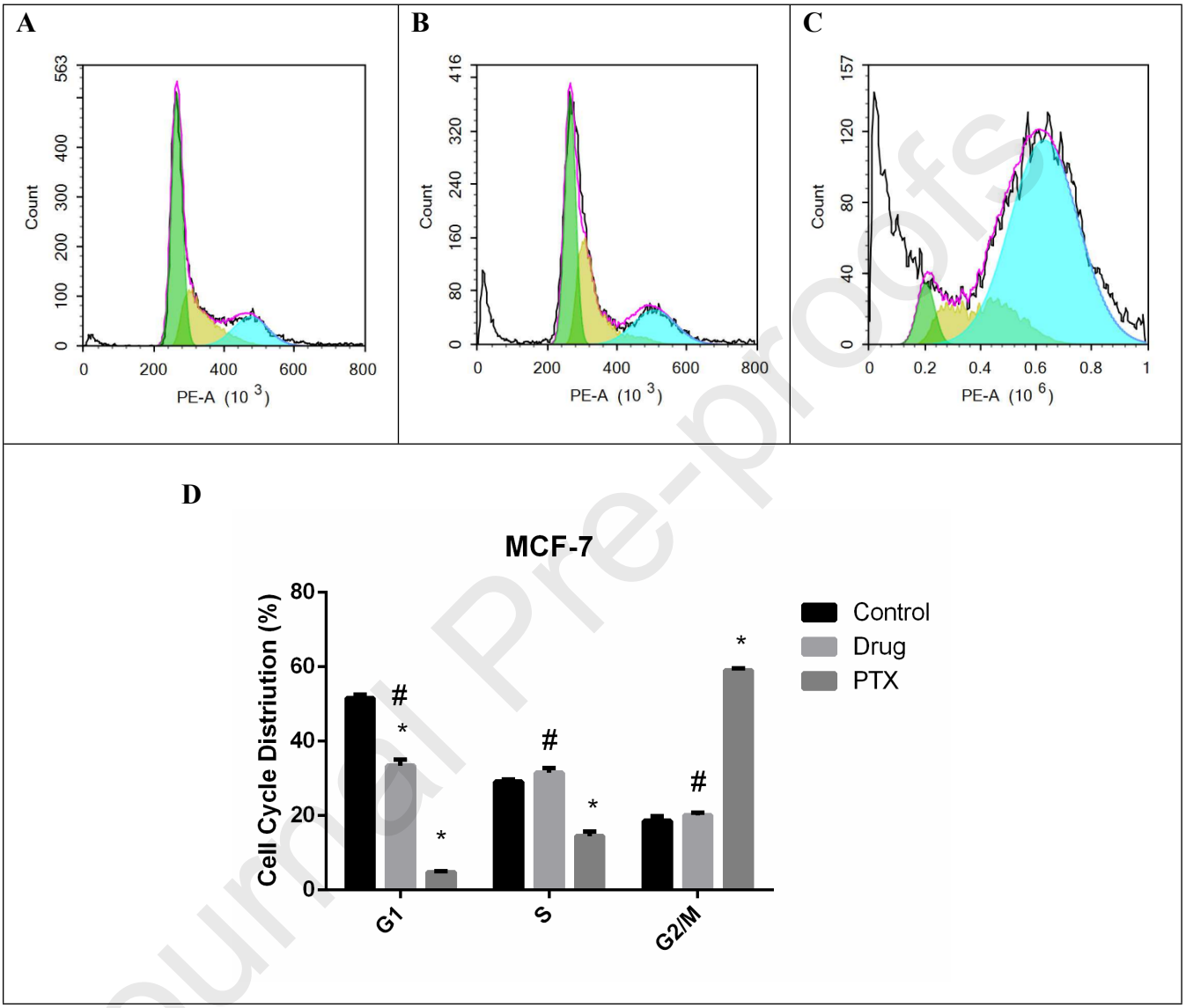

Figure 2. Cell cycle analysis in MCF-7 cells.Cells were subjected to cell cycle analysis using flow cytometry. Representative histogram of the gated cells in the G0/G1, S, and G2/M phases for A: control; B: Compound 11i; C: PTX. D: Quantitative analysis of distribution or proportion of the cells in each phase was performed from at least 10,000 cells per sample. Each bar represents mean ± SEM of the data obtained from three independent experiments. *p < 0.05 vs. control

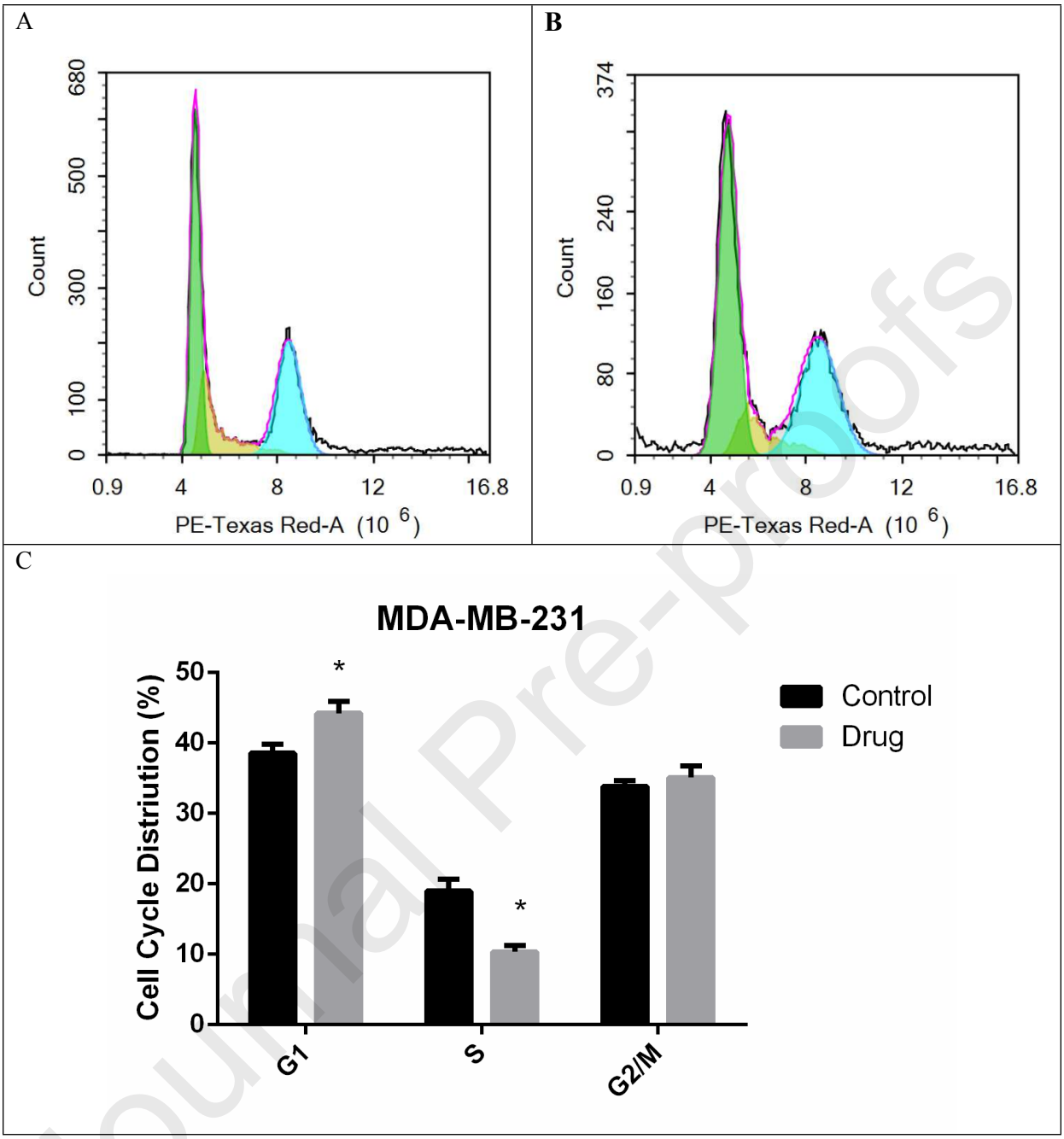

Figure 3. Cell cycle analysis in MDA-Mb-231 cells. Cells were subjected to cell cycle analysis using flow cytometry. Representative histogram of the gated cells in the G0/G1, S, and G2/M phases for A: control; B: Compound 11i. C: Quantitative analysis of distribution or proportion of the cells in each phase was performed from at least 10,000 cells per sample. Each bar represents mean ± SEM of the data obtained from three independent experiments. *$p < 0.05$ vs. control.

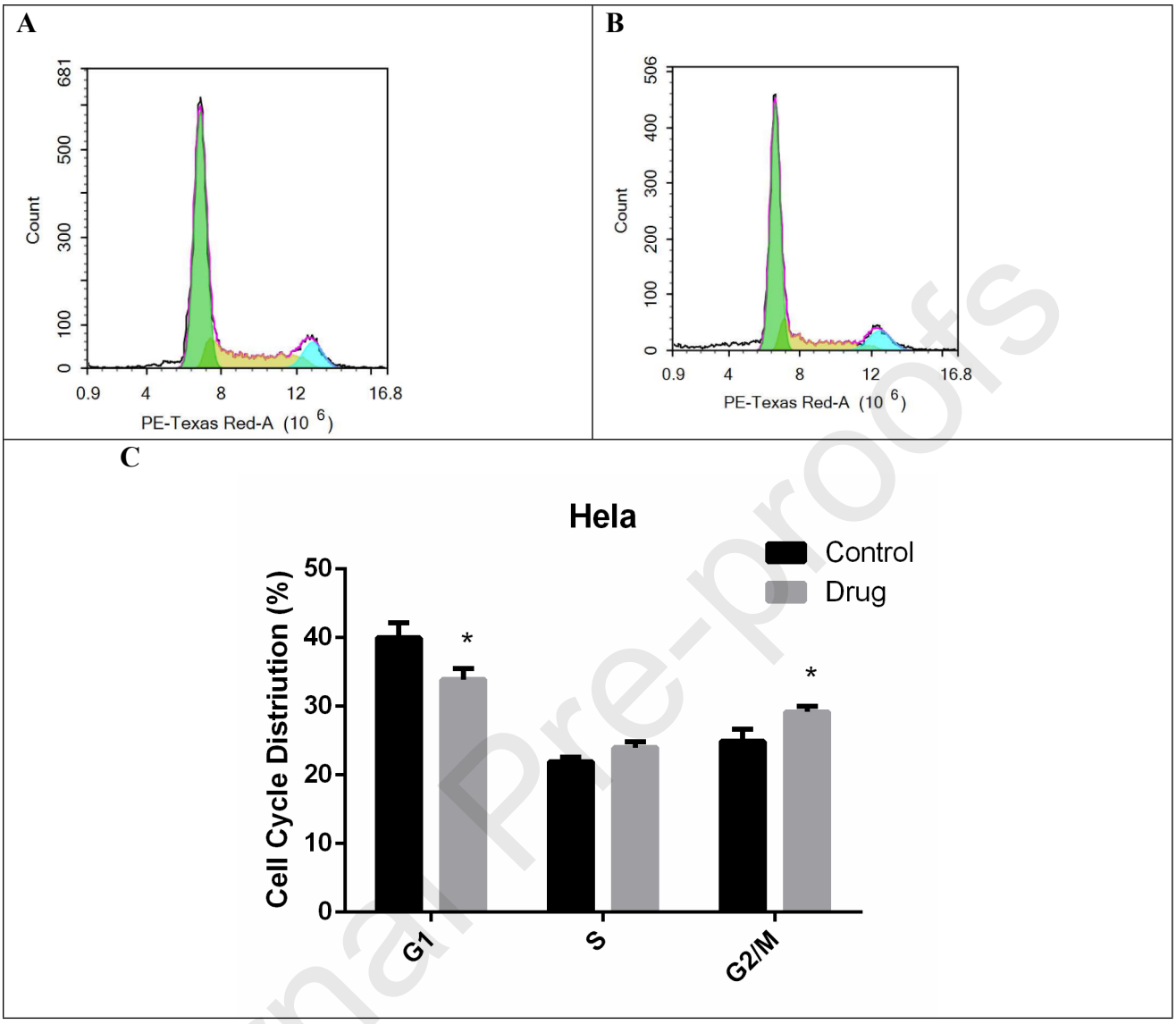

Figure 4. Cell cycle analysis in Hela cells. Cells were subjected to cell cycle analysis using flow cytometry. Representative histogram of the gated cells in the G0/G1, S, and G2/M phases for A: control; B: Compound 16b. C: Quantitative analysis of distribution or proportion of the cells in each phase was performed from at least 10,000 cells per sample. Each bar represents mean ± SEM of the data obtained from three independent experiments. *p < 0.05 vs. control.

2.2.5. In-silico ADME study

Computer aided ADME study was performed by using the software: Swiss ADME tool. These studies are based on the chemical structure of the molecule and involves the calculation of certain parameters including; human gastrointestinal absorption (HIA) and blood-brain barrier (BBB) permeation both consist in the readout of the BOILED-Egg model substrate or non-

substrate of the permeability glycoprotein (P-gp), interaction of molecules with cytochromes P450 (CYP) and bioavailability score also calculate the molecular properties of the ligands following the Lipinski rule of five (5), molar refractivity, The total polar surface area (TPSA) and The partition coefficient between n-octanol and water (log Po/w).

2.2.5.1. Results of the ADME study

The results of the ADME study are presented as BOILIED-EGG, which is a 2D plot drawn using calculated TPSA and A WLOGP properties. Blood Brain Barrier (BBB) and Human Intestinal Absorption (HIA) plots were drawn using all the compounds. (Fig 5).

In BBB plot, showed nine of the newly synthesized compounds fell inside the yolk which may be able to penetrate the blood brain barrier and seven of these compounds fell outside the yolk which may not be able to penetrate the blood brain barrier which indicate that the chances of CNS side effects in these seven compounds are predicted to be low. In HIA plot, all the synthesized compounds fell inside the white, which indicate all compounds have excellent human intestinal absorption.

ADME Aqueous solubility level of most of the compounds was found to be moderate solubility.

The CYP2D6 score predicts the inhibitory and non-inhibitory character of the given chemical structure on Cytochrome P450 2D6 enzyme. Most of the compounds are predicted as inhibitors of CYP2D6. The calculated parameters from the ADMET study are tabulated in (Table 3).

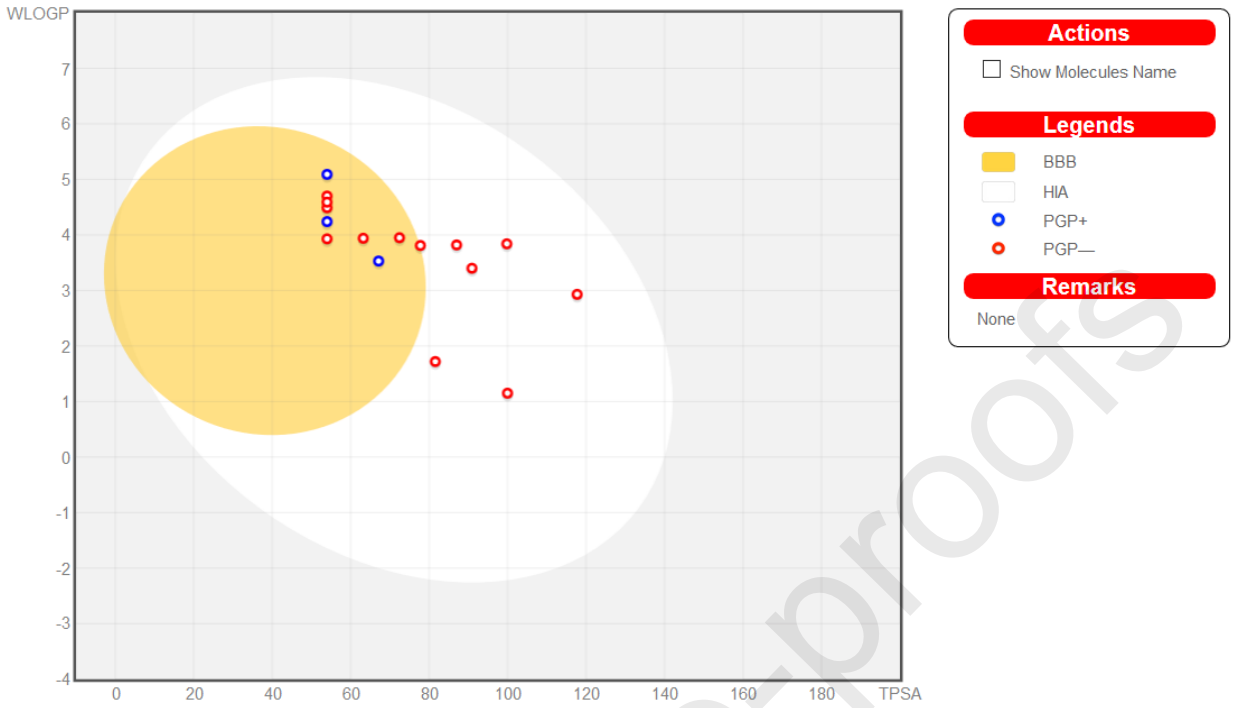

Figure 5. The BOILED-Egg chart for the synthesized compounds developed by swiss ADME.

Table 3. Computer aided ADME screening of the synthesized compounds:

	Parameters									
CPD ID	**GI Absorption**	**BBB permeation**	**Pg-p substrate**	**CYP1A2 inhibitor**	**CYP2C19 inhibitor**	**CYP2C9 inhibitor**	**CYP2D6 inhibitor**	**CYP3A4 inhibitor**	**Logkp (Skin permeation)**	**Bioavailability score**
11a	High	Yes	No	Yes	Yes	Yes	Yes	Yes	-5.71	0.55
11b	High	Yes	Yes	Yes	Yes	Yes	Yes	Yes	-5.54	0.55
11c	High	Yes	No	Yes	Yes	Yes	Yes	Yes	-5.92	0.55
11d	High	Yes	No	Yes	Yes	Yes	Yes	Yes	-6.12	0.55
11e	High	Yes	No	Yes	Yes	Yes	Yes	Yes	-5.75	0.55
11f	High	Yes	No	Yes	Yes	Yes	Yes	Yes	-5.48	0.55
11g	High	Yes	No	Yes	Yes	Yes	Yes	No	-5.71	0.55
11h	High	No	No	Yes	Yes	Yes	No	No	-6.11	0.55
11i	High	Yes	Yes	Yes	Yes	Yes	Yes	No	-5.13	0.55
11j	High	Yes	Yes	Yes	Yes	Yes	Yes	Yes	-6.29	0.55
16a	High	No	No	Yes	Yes	Yes	Yes	Yes	-6.07	0.55
16b	High	No	No	Yes	No	Yes	Yes	Yes	-6.27	0.55
16c	High	No	No	Yes	No	Yes	Yes	Yes	-6.64	0.55

22	High	No	No	Yes	No	No	No	No	-7.39	0.55
23	High	No	No	Yes	No	No	No	No	-6.5	0.55
25	High	No	No	Yes	Yes	Yes	No	No	-5.45	0.55

2.2.5.2. Prediction of toxicity

Protox-II server [24] was used to predict the organ toxicities and toxicological end points of the ligands and their LD50. The integrated PubChem search (https:/pubchem.ncbi.nlm.nih.gov/) was used to search for chemical structures using the compound names. The models to be used were selected and the webserver computed the acute toxicity and toxicity targets selected.

The prediction of toxicity was based on 6 different targets linked to adverse drug-reactions. The hepatotoxicity, carcinogenicity, immunotoxicity, mutagenicity and cytotoxicity of the compounds were determined. All compounds are found to have hepatotoxicity except compound **11f**. Compounds **11d**, **11h**, **22**, **23** and **25** are found to be carcinogenic, also compounds **11**h and **25** are found to have mutagenicity. The acute toxicity of the ligands was checked using PROTOX -II server. All compounds with LD_{50} of 300 mg/kg have class 3 except compound (**23** and **25**) have class 4 with LD_{50} of 600 mg/kg and 2000 mg/kg, respectively (Table 4).

Table 4. Toxicity prediction of the synthesized compounds

	Predicted target					
Compound	**Hepatotoxicity**	**Carcinogenicity**	**Immunotoxicity**	**Mutagenicity**	**Cytotoxicity**	**Acute toxicity**
11a	Active	Inactive	Inactive	Inactive	Inactive	Class 3
11b	Active	Inactive	Inactive	Inactive	Inactive	Class 3
11c	Active	Inactive	Inactive	Inactive	Inactive	Class 3
11d	Active	Active	Inactive	Inactive	Inactive	Class 3
11e	Active	Inactive	Inactive	Inactive	Inactive	Class 3
11f	Inactive	Inactive	Inactive	Inactive	Inactive	Class 3
11g	Active	Inactive	Inactive	Inactive	Inactive	Class 3
11h	Active	Active	Inactive	Active	Inactive	Class 3
11i	Active	Inactive	Inactive	Inactive	Inactive	Class 3
11j	Active	Inactive	Inactive	Inactive	Inactive	Class 3
16a	Active	Inactive	Inactive	Inactive	Inactive	Class 3

16b	Active	Inactive	Inactive	Inactive	Inactive	Class 3
16c	Active	Inactive	Inactive	Inactive	Inactive	Class 3
22	Active	Active	Inactive	Inactive	Inactive	Class 3
23	Active	Active	Inactive	Inactive	Inactive	Class 4
25	Active	Active	Inactive	Active	Inactive	Class 4

3. Conclusion

A series of pyrazolo[1,5-*a*]pyrimidines **11a-j**, **16a-c**, **22** in addition to acetamide **23** and hydrazone **25** were synthesized. Compounds **11f**, **16b** and **11i** emerged as the most active compounds towards Huh-7, HeLa and MCF-7 cell lines with IC_{50} = 6.3, 7.8 and 3.0 μM, respectively. Compounds **11i** and **16b** showed potent antiproliferative activity with IC_{50} = 4.32 μM and 5.74 μM, respectively, against the MDA-MB231 cell lines. Cell cycle analysis of **11i** induced a reduction in G1 phase with arrest in S phase and G2/M phase when treated with MCF-7 cells. Compound **16b** induced a reduction in G1 phase and arrest in G2/M phase when treated with Hela cells. Compound **11i** induced arrest in G1 phase and reduction in S phase when treated with MDA-MB-231 cells. Taken together, these compounds may act as promising hits for further development of new antiproliferative agents.

4. Experimental

4.1. Chemistry

Melting points (°C, uncorrected) were determined using a Stuart melting point apparatus. The IR spectra (KBr) were recorded on a SHIMADZU FT/IR spectrometer. The NMR spectra recorded by BRUKER 400 MHz NMR spectrometers use DMSO-d_6 as solvent. Chemical shifts were reported in parts per million (δ), and coupling constants (J) expressed in Hertz. TMS was used as an internal standard and chemical shifts were measured in δ ppm. ^{1}H and ^{13}C spectra were run at 400 and 100 MHz, respectively. Electron impact mass spectra were measured on Direct probe controller inlet part to single quadropole mass analyzer in THERMO SCIENTIFIC GCMS model (ISQ LT) using THERMO X-CALIBUR SOFTWARE at the regional center for mycology and biotechnology (RCMB) Al-azhar University, Naser city, Cairo.

*4.1.1. Synthesis of 3-amino-2-benzoyl-4,4,4-trichlorobut-2-enenitrile (**2**)*

To a stirred solution of 3-oxo-3-phenylpropanenitrile (**1**) (1.45 g, 10 mmol) in EtOH (20 mL) and in the presence of anhydrous AcONa (1.0 g), 3,3,3-trichloropropanenitrile (10 mmol, 1.57 g), was added. The resulting mixture was stirred for 6 h at rt., and then the solvent was evaporated under vacuum to half of its volume. The reaction mixture was then poured into water. The solid product obtained was collected by filtration and recrystallization from ethanol to give compound **2** as pale yellow crystals in 80 % yield, mp 182^{o}C (Let. mp 182-184^{o}C, [25]).

*4.1.2. 5-Amino-3-phenyl-1H-pyrazole-4-carbonitrile (**3**)*

"A mixture of compound **2** (2.90 g, 10 mmol) and hydrazine hydrate (80%, 3 mL) in dioxane (20 mL) was refluxed for 30 min. The reaction mixture is then allowed to cool at ambient temperature. The precipitate was filtered off and recrystallized from ethanol from ethanol to give compound 3. The physical properties of **3** were identical to those reported for compound **3** as buff crystals in 86 % yield, mp 200^{o}C (Let. mp 200-202^{o}C, [25]).

*4.1.3. Synthesis of 3-(dimethylamino)-1-arylprop-2-en-1-ones **6a-j***

To a solution of aryl ethenone **4a-j** (20 mmol) in xylene (50 mL), dimethylformamide-dimethylacetal (**5**) (2.38 g, 20 mmol), was added and then the reaction was refluxed for 7 h. The xylene was distilled off and the product was triturated with diethyl ether (5 mL). The resulting solid was filtered and washed with cold petroleum ether to afford the pure compounds **6a-j**, respectively. The physical properties of **6a-j** were identical to those reported [19-22].

*4.1.4. Synthesis of 7-(aryl)-2-phenylpyrazolo[1,5-a]pyrimidine-3-carbonitrile **11a-j***

A mixture of the appropriate enaminone **6a-j** (10 mmol) and 5-amino-3-phenyl-1*H*-pyrazole-4-carbonitrile (**3**) (1.84 g, 10 mmol) in acetic acid (25 mL) was refluxed for 3 h, then left to cool. The solid product filtered off, washed with ethanol, dried and finally recrystallized from dimethylformamide/H_2O to afford the corresponding **11a-j**, respectively.

*4.1.4.1. 2,7-Diphenylpyrazolo[1,5-a]pyrimidine-3-carbonitrile (**11a**)*

White powder, 55% yield; mp 210-211°C; IR (KBr) ν_{max}/cm^{-1} 3150 (Aromatic CH), 2225 (C≡N), 1610 (C=N); ^{1}H NMR δ 7.63-7.64 (m, 4H, H3, H3`, H4 of phenyl of pyrazole and H3 of pyrimidine), 7.65-7.71 (m, 3H, H3, H3` and H4 of phenyl of pyrimidine), 8.04-8.07 (m, 2H, H2 and H2` of phenyl of pyrazole), 8.17-8.20 (m, 2H, H2 and H2` of phenyl of pyrimidine), 8.88 (d, J = 5.6 Hz, 1H, H2 of pyrimidine); ^{13}C NMR δ 79.02 (C4 of pyrazole), 111.59, 114.75, 127.56 (2C), 129.14 (2C), 129.72 (2C), 129.91 (2C), 130.27, 130.60, 131.08, 132.22, 147.67, 153.25, 154.10, 156.09. MS *m/z* (%) 297.24 (M^++1, 22.21), 296.22 (M^+, 100); Anal. Calcd. For: $C_{19}H_{12}N_4$ (296.33): C, 77.01; H, 4.08; N, 18.91; Found: C, 76.89; H, 4.25; N, 19.17.

*4.1.4.2. 2-Phenyl-7-(p-tolyl)pyrazolo[1,5-a]pyrimidine-3-carbonitrile (**11b**)*

White powder, 60% yield; mp 220-222°C; IR (KBr) ν_{max}/cm^{-1} 3100 (Aromatic CH), 2900 (Aliphatic CH), 2225 (C≡N), 1625 (C=N); ^{1}H NMR (DMSO-d_6) δ 2.44 (s, 3H, C<u>H</u>$_3$), 7.44 (d, J = 8.8 Hz, 2H, H3, H3` of Aryl), 7.54-7.61 (m, 4H, H3, H3`, H4 of phenyl and H3 pyrimidine), 8.04-8.05 (m, 2H, H2 and H2` of phenyl), 8.08 (d, $J$ = 9.6 Hz, 2H, H2 and H2` of aryl), 8.83 (d, J = 4.4 Hz, 1H, H2 of pyrimidine); ^{13}C NMR (DMSO-d_6) δ 21.59 (-<u>C</u>H$_3$), 78.87 (C4 of pyrazole), 111.11, 114.77, 126.95, 127.52 (2C), 129.69 (3C), 130.19 (2C), 130.62 (2C), 131.04, 142.52, 147.65, 153.29, 153.93, 155.97. MS *m/z* (%) 311.31 (M^++1, 9.73), 310.27 (M^+, 58.26), 77.19 (100), 51.16 (44.52); Anal. Calcd. For: $C_{20}H_{14}N_4$ (310.35): C, 77.40; H, 4.55; N, 18.05; Found: C, 77.68; H, 4.69; N, 18.31.

*4.1.4.3. 7-(4-Methoxyphenyl)-2-phenylpyrazolo[1,5-a]pyrimidine-3-carbonitrile (**11c**)*

Buff powder, 58% yield; mp 184-185°C; IR (KBr) ν_{max}/cm^{-1} 3100 (Aromatic CH), 2850 (Aliphatic CH), 2224 (C≡N), 1620 (C=N); ^{1}H NMR δ 3.88 (s, 3H, OC<u>H</u>$_3$), 7.16 (d, J = 6.8 Hz, 2H, H3, H3`of aryl), 7.52 (d, $J$ = 6.8 Hz, 1H, H3 of pyrimidine), 7.55-7.60 (m, 3H, H3, H3` and H4 of phenyl), 8.04-8.05 (m, 2H, H2 and H2` of phenyl), 8.22 (d, $J$ = 9.6 Hz, 2H, H2, H2` of aryl), 8.78 (d, J = 5.6 Hz, 1H, H2 of pyrimidine); ^{13}C NMR δ 56.01 (O<u>C</u>H$_3$), 78.70 (C4 of pyrazole), 110.46, 114.57 (2C), 114.81, 121.68, 127.49 (2C), 129.64 (2C), 130.63, 131.01, 132.18 (2C), 147.22, 153.39, 153.67, 155.86, 162.48. MS *m/z* (%) 327.27 (M^++1, 21.01), 326.27 (M^+, 100), 77.14 (93.68); Anal. Calcd. For: $C_{20}H_{12}N_4O$ (326.35): C, 73.61; H, 4.32; N, 17.17; Found: C, 73.89; H, 4.60; N, 17.40.

*4.1.4.4. 7-(3,4-Dimethoxyphenyl)-2-phenylpyrazolo[1,5-a]pyrimidine-3-carbonitrile (**11d**)*

Buff powder, 62% yield; mp 220-221°C; IR (KBr) ν_{max}/cm^{-1} 3100 (Aromatic CH), 2850 (Aliphatic CH), 2226 (C≡N), 1620 (C=N); ^{1}H NMR δ 3.88 (s, 3H, OC$\underline{H}_3$), 3.90 (s, 3H, OC$\underline{H}_3$), 7.21 (d, J = 6.8 Hz, 1H, H5 of aryl), 7.55-7.64 (m, 4H, H3, H3`, H4 of phenyl and H3 of pyrimidine), 7.89 (s, 1H, H2 of aryl), 7.92 (d, $J$ = 8.4 Hz, 1H, H6 of aryl), 8.07 (d, $J$ = 8.4 Hz, 2H, H2, H2` of phenyl), 8.81 (d, J = 6 Hz, 1H, H2 of pyrimidine); ^{13}C NMR δ 56.19 (O$\underline{C}$H$_3$), 56.23 (O$\underline{C}$H$_3$), 78.66 (C4 of pyrazole), 110.64, 111.90, 113.50, 114.86, 121.66, 124.15, 127.44 (2C), 129.74 (2C), 130.69, 131.07, 147.27, 148.77, 152.31, 153.49, 153.69, 155.83. MS *m/z* (*%*) 357.30 (M$^+$+1, 25.77), 356.28 (M$^+$, 100); Anal. Calcd. For: $C_{21}H_{16}N_4O_2$ (356.38): C, 70.77; H, 4.53; N, 15.72; Found: C, 70.85; H, 4.76; N, 15.94.

*4.1.4.5. 7-(4-Fluorophenyl)-2-phenylpyrazolo[1,5-a]pyrimidine-3-carbonitrile (**11e**)*

White powder, 65% yield; mp 250-252°C; IR (KBr) ν_{max}/cm^{-1} 3100 (Aromatic CH), 2230 (C≡N), 1600 (C=N); ^{1}H NMR δ 7.49-7.54 (m, 2H, H3, H3` of aryl), 7.57-7.63 (m, 4H, H3, H3`,H4 of phenyl and H3 of pyrimidine), 8.05-8.07 (m, 2H, H2 and H2` of phenyl), 8.27-8.31 (m, 2H, H2 and H2` of aryl), 8.89 (d, J = 4.4 Hz, 1H, H2 of pyrimidine); ^{13}C NMR δ 79.04 (C4 of pyrazole), 111.51, 114.72, 116.19, 116.41, 126.34, 127.56 (3C), 129.72 (3C), 130.57, 131.11, 133.03, 133.12, 146.67, 153.24, 154.06, 156.06. MS *m/z* (*%*) 315.22 (M$^+$+1, 20.92), 314.20 (M$^+$, 100), 77.13 (95.33); Anal. Calcd. For: $C_{19}H_{11}N_4$ (314.32): C, 72.60; H, 3.53; N, 17.83; Found: C, 72.84; H, 3.67; N, 18.19.

*4.1.4.6. 7-(4-Chlorophenyl)-2-phenylpyrazolo[1,5-a]pyrimidine-3-carbonitrile (**11f**)*

Buff powder, 78% yield; mp 271-273°C; IR (KBr) ν_{max}/cm^{-1} 3100 (Aromatic CH), 2225 (C≡N), 1625 (C=N); ^{1}H NMR δ 7.59-7.62 (m, 4H, H3, H3`, H4 of phenyl and H3 of pyrimidine), 7.73 (d, , $J$ = 9.2 Hz, 2H, H3, H3` of aryl), 8.04 (d, J = 8.8 Hz, 2H, H2 and H2` of phenyl), 8.21 (d, $J$ = 8.8 Hz, 2H, H2 and H2` of aryl), 8.89 (d, J = 5.2 Hz, 1H, H2 of pyrimidine); ^{13}C NMR δ 79.13 (C4 of pyrazole), 111.63, 115.01, 127.61 (3C), 129.29 (3C), 129.76 (3C), 131.16, 132.20 (3C), 137.04, 154.15, 187.96. MS *m/z* (*%*) 331.21 (M$^+$+1, 35.70), 330.18 (M$^+$, 100);Anal. Calcd. For: $C_{19}H_{11}N_4$ (330.77): C, 68.99; H, 3.35; N, 16.94; Found: C, 69.21; H, 3.59; N, 17.12.

*4.1.4.7. 7-(4-Bromophenyl)-2-phenylpyrazolo[1,5-a]pyrimidine-3-carbonitrile (**11g**)*

Off white powder, 70% yield; mp 260-261°C; IR (KBr) ν_{max}/cm^{-1} 3100 (Aromatic CH), 2900 (Aliphatic CH), 2227 (C≡N), 1610 (C=N); ^{1}H NMR δ 7.54-7.62 (m, 4H, H3, H3`, H4 of phenyl and H3 of pyrimidine), 7.86 (d, $J$ = 8 Hz, 2H, H3 and H3` of aryl), 8.05-8.06 (m, 2H, H2 and H2` of phenyl), 8.13 (d, $J$ = 9.6 Hz, 2H, H2 and H2` of aryl), 8.88 (d, J = 6 Hz, 1H, H2 of pyrimidine); ^{13}C NMR δ 79.10 (C4 of pyrazole), 111.56, 114.69, 125.98, 127.56 (2C), 129.04, 129.72 (2C), 130.52, 131.13, 132.20 (2C), 132.28 (2C), 146.60, 153.20, 154.10, 156.05. MS *m/z* (*%*) 376.19 (M$^+$+2, 93.50), 375.22 (M$^+$+1, 54.67), 374.21 (M$^+$, 94.46), 77.13 (100);Anal. Calcd. For: $C_{19}H_{11}N_4$ (375.22): C, 60.82; H, 2.95; N, 14.93; Found: C, 61.06; H, 3.11; N, 15.20.

*4.1.4.8. 7-(4-Nitrophenyl)-2-phenylpyrazolo[1,5-a]pyrimidine-3-carbonitrile (**11h**)*

Pale yellow, 68% yield; mp 290-291°C; IR (KBr) ν_{max}/cm^{-1} 3100 (Aromatic CH), 2220 (C≡N), 1600 (C=N), 1350-1360 (NO_2); ^{1}H NMR δ 7.59-7.60 (m, 3H, H3, H3`and H4 of phenyl), 7.70 (d, $J$ = 4.8 Hz, 1H, H3 of pyrimidine), 8.06-8.07 (m, 2H, H2 and H2` of phenyl), 8.42 (d, J = 9.6 Hz, 2H, H2 and H2` of aryl), 8.47 (d, $J$ = 8.8 Hz, 2H, H3 and H3` of aryl), 8.96 (d, J = 5.6 Hz, 1H, H2 of pyrimidine); ^{13}C NMR δ 73.52, 79.35 (C4 of pyrazole), 112.40, 114.59, 124.08 (2C), 127.58, 129.74 (2C), 130.42, 131.20, 131.87 (C2), 135.89, 145.58, 149.42, 153.11, 154.26, 156.16. MS *m/z* (*%*) 342.33 (M$^+$+1, 16.29), 341.28 (M$^+$, 100); Anal. Calcd. For: $C_{19}H_{11}N_5O_2$ (341.32): C, 66.86; H, 3.25; N, 20.52; Found: C, 67.12; H, 3.49; N, 20.36.

*4.1.4.9. 7-(Naphthalen-2-yl)-2-phenylpyrazolo[1,5-a]pyrimidine-3-carbonitrile (**11i**)*

Buff powder, 70% yield; mp 226-228°C; IR (KBr) ν_{max}/cm^{-1} 3100 (Aromatic CH), 2223 (C≡N), 1620 (C=N); ^{1}H NMR δ 7.60-7.62 (m, 3H, H3, H3`and H4 of phenyl), 7.65-7.71 (m, 3H, naphthalene Hs and H3 of pyrimidine), 8.03-8.07 (m, 3H, H2, H2` of phenyl and 1H of naphthalene), 8.10-8.14 (m, 2H, naphthalene Hs), 8.20-8.23 (m, 1H, naphthalene H), 8.80 (s, 1H, H1 of naphthalene), 8.90 (d, J = 5.6 Hz, 1H, H2 of pyrimidine); ^{13}C NMR δ 79.05 (C4 of pyrazole), 111.84, 114.77, 126.33, 127.33, 127.56 (3C), 128.15, 128.46, 128.84, 129.53 (2C), 129.71, 130.60, 131.07, 131.11, 132.65, 134.50, 147.58, 153.29, 154.02, 156.10. MS *m/z* (*%*) 347.27 (M$^+$+1, 25.61), 346.25 (M$^+$, 100), 345.25 (60.43); Anal. Calcd. For: $C_{23}H_{14}N_4$ (346.38): C, 79.75; H, 4.07; N, 16.17; Found: C, 79.91; H, 4.23; N, 16.45.

*4.1.4.10. 7-(Furan-2-yl)-2-phenylpyrazolo[1,5-a]pyrimidine-3-carbonitrile (**11j**)*

Brown powder, 62% yield; mp 204-206°C; IR (KBr) ν_{max}/cm^{-1} 3150 (Aromatic CH), 2225 (2C≡N), 1575 (C=N); ^{1}H NMR δ 6.97 (s, 1H, H4 of furan), 7.58-7.65 (m, 3H, H3, H3` and H4 of phenyl), 7.68 (d, $J$ = 6.4 Hz, 1H, H3 of pyrimidine), 8.18 (d, $J$ = 5.6 Hz, 2H, H2 and H2` of phenyl), 8.26 (s, 2H, H3 and H5 of furan), 8.82 (d, J = 4.4 Hz, 1H, H2 of pyrimidine); ^{13}C NMR δ 78.83 (C4 of pyrazole), 106.13, 114.38, 114.71, 121.84, 127.57 (2C), 129.79 (2C), 130.47, 131.25, 136.46, 142.71, 148.90, 152.83, 153.27, 156.32. MS *m/z* (%) 287.21 (M^++1, 14.93), 286.21 (M^+, 66.07), 77.14 (100); Anal. Calcd. For: $C_{17}H_{10}N_4O$ (286.29): C, 71.32; H, 3.52; N, 19.57; Found: C, 71.08; H, 3.80; N, 19.71.

*4.1.5. Synthesis of 2-Aryl-3-(dimethylamino)acrylonitrile **12a-c***

To a mixture of 3-(aryl)-3-oxopropanenitrile **3a-c** (20 mmol), in xylene (50 mL), was added dimethylformamide-dimethylacetal (2.38 g, 20 mmol) and the reaction refluxed for 1 h. The xylene was distilled off and the product was triturated with petroleum ether. The resulting solid was filtered and washed with cold petroleum ether to afford the pure compounds **12a-c**, respectively. The physical properties of **12a-c** were identical to those reported [25-26]).

*4.1.6. Synthesis of 2-Phenyl-7-(aryl)pyrazolo[1,5-a]pyrimidine-3,6-dicarbonitrile **16a-c***

A mixture of the appropriate enaminone **12a-c** (10 mmol) and 5-amino-3-phenyl-1*H*-pyrazole-4-carbonitrile (**3**) (1.84 g, 10 mmol) in acetic acid (25 mL) was refluxed for 3 h, then left to cool. The solid product filtered off, washed with ethanol, dried and finally recrystallized from dimethylformamide/H_2O to give the corresponding 2-phenyl-7-(aryl)pyrazolo[1,5-*a*]pyrimidine-3,6-dicarbonitriles **16a-c**, respectively.

*4.1.6.1. 2,7-Diphenylpyrazolo[1,5-a]pyrimidine-3,6-dicarbonitrile (**16a**)*

Yellow powder, 42% yield; mp 229-230°C; IR (KBr) ν_{max}/cm^{-1} 3100 (Aromatic CH), 2240 (2C≡N), 1610 (C=N); ^{1}H NMR δ 7.59-7.64 (m, 3H, H3, H3`and H4 of phenyl of pyrimidine), 7.71-7.80 (m, 3H, H3, H3` and H4 of phenyl of pyrazole), 7.99-8.01 (m, 4H, H2, H2` of phenyl of pyrazole, H2 and H2` of phenyl of pyrimidine), 9.25 (s, 1H, H2 of pyrimidine); ^{13}C NMR δ 81.30 (C4 of pyrazole), 98.47 (C3 of pyrimidine), 113.79, 115.49, 127.27, 127.65 (2C), 129.17,

129.36 (2C), 129.50, 129.74, 129.88, 130.73, 131.70, 133.14, 153.09, 153.29, 154.87, 157.98; Anal. Calcd. For: $C_{20}H_{11}N_5$ (321.33): C, 74.76; H, 3.45; N, 21.79; Found: C, 74.90; H, 3.66; N, 21.57.

*4.1.6.2. 7-(4-Methoxyphenyl)-2-phenylpyrazolo[1,5-a]pyrimidine-3,6-dicarbonitrile (**16b**)*

Yellow powder, 40% yield; mp > 300°C; IR (KBr) ν_{max}/cm^{-1} 3400 (Aromatic CH), 2900 (Aliphatic CH), 2230 (2C≡N), 1520 (C=N); ^{1}H NMR δ 3.92 (s, 3H, OC<u>H</u>$_3$), 7.24 (d, J = 8.8 Hz, 2H, H3 and H3` of aryl), 7.63-7.66 (m, 3H, H3, H3` and H4 of phenyl), 7.87-7.89 (m, 2H, H2 and H2` of phenyl), 8.15 (d, $J$ = 7.4 Hz, 2H, H2 and H2` of aryl), 9.04 (s, 1H, H2 of pyrimidine). MS *m/z* (*%*) 351.12 (M$^+$, 7.60), 77.07 (100); Anal. Calcd. For: $C_{21}H_{13}N_5O$ (351.36): C, 71.79; H, 3.73; N, 19.93; Found: C, 72.04; H, 3.87; N, 20.16.

*4.1.6.3. 7-(Furan-2-yl)-2-phenylpyrazolo[1,5-a]pyrimidine-3,6-dicarbonitrile (**16c**)*

Brown powder, 69% yield; mp 265-267°C; IR (KBr) ν_{max}/cm^{-1} 3200 (Aromatic CH), 2230 (2C≡N), 1610 (C=N); ^{1}H NMR δ 7.11 (d, J = 4 Hz, 1H, H4 of furan), 7.60-7.66 (m, 3H, H3, H3` and H4 of phenyl), 8.18-8.19 (m, 2H, H2 and H2` of phenyl), 8.49 (s, 1H, H3 of furan), 8.55-8.57 (d, J = 4.4 Hz, 1H, H5 of furan), 9.11 (s, 1H, H2 of pyrimidine); ^{13}C NMR δ 80.93 (C4 of pyrazole), 92.26 (C3 of pyrimidine), 113.81, 115.30, 115.92, 127.10, 127.69 (2C), 129.68, 129.95 (2C), 131.84, 139.09, 141.31, 150.76, 153.03, 155.43, 157.61. MS *m/z* (*%*) 312.17 (M$^+$+1, 22.68), 311.15 (M$^+$, 100); Anal. Calcd. For: $C_{18}H_9N_5O$ (311.30): C, 69.45; H, 2.91; N, 22.50; Found: C, 69.18; H, 3.24; N, 22.37.

*4.1.7. Synthesis of 7-Amino-5-oxo-2-phenyl-4,5-dihydropyrazolo[1,5-a]pyrimidine-3-carbonitrile (**22**)*

A mixture of compound **3** (0.18 g, 1 mmol) and ethyl cyanoacetate (**19**) (0.113 g, 1 mmol) was heated to reflux for 45 min. and then left to cool at r.t. Ethanol (5 mL) was added, the solid separated was collected by filtration, washed with ethanol, and finally recrystallized from EtOH/DMF to afford compound **22** as light brown powder, 75% yield; mp > 300°C; IR (KBr) ν_{max}/cm^{-1} 3150-3400 (NH, NH$_2$), 3100 (Aromatic CH), 2220 (C≡N), 1680 (C=O), 1630 (C=N); ^{1}H NMR δ 5.41 (s, 1H, C<u>H</u> pyrimidine), 7.51-7.59 (m, 3H, H3, H3` and H4 of phenyl), 7.77 (s, D$_2$O exchangeable, 2H, N<u>H$_2$</u>), 8.01-8.03 (m, 2H, H2 and H2` of phenyl), 12.07 (br. s, D$_2$O

exchangeable, 1H, NH); ^{13}C NMR δ 77.82 (C4 of pyrazole), 115.46, 127.27 (3C), 129.42 (3C), 130.53, 131.09, 150.21, 154.20, 164.90. MS *m/z* (*%*) 252.18 (M^++1, 2.45), 251.19 (M^+, 10.87), 68.11 (100); Anal. Calcd. For: $C_{13}H_9N_5O$ (251.24): C, 62.15; H, 3.61; N, 27.87; Found: C, 62.37; H, 3.89; N, 27.61.

*4.1.8. Synthesis of N-(4-cyano-3-phenyl-1H-pyrazol-5-yl)acetamide (**23**)*

A solution of compound **3** (1.84 g, 10 mmol) in acetic acid (25 mL) was refluxed for 2 h, and then left to cool. The solid product filtered off, washed with ethanol, dried and finally recrystallized from DMF/H_2O to gave the corresponding *N*-(4-cyano-3-phenyl-1*H*-pyrazol-5-yl)acetamide (**23**) as buff powder in 40% yield; mp 290-293^{o}C; IR (KBr) ν_{max}/cm^{-1} 3225, 3235 (2NH), 3150 (Aromatic CH), 2900 (Aliphatic CH), 2228 (C≡N), 1700 (C=O), 1620 (C=N); ^{1}H NMR δ 2.10 (s, 3H, CH_3), 7.50-7.59 (m, 3H, H3, H3`and H4 of phenyl), 7.82-7.84 (m, 2H, H2 and H2` of phenyl), 10.73 (br. s, D_2O exchangeable, 1H, NHCOMe), 13.67 (br. s, D_2O exchangeable, 1H, NH of pyrazole); ^{13}C NMR δ 23.15 (CH_3), 114.79, 126.75 (3C), 129.67 (3C), 130.31, 169.42, 196.70. MS *m/z* (*%*) 227.21 (M^++1, 1.07), 226.18 (M^+, 21.04), 77.15 (100); Anal. Calcd. For: $C_{12}H_{10}N_4O$ (226.23): C, 63.71; H, 4.46; N, 24.76; Found: C, 63.54; H, 4.70; N, 24.89.

*4.1.9. Synthesis of N-(4-cyano-3-phenyl-1H-pyrazol-5-yl)-2-oxo-2-phenylacetohydrazonoyl cyanide (**25**)*

A solution of 5-amino-3-phenyl-1*H*-pyrazole-4-carbonitrile (**3**) (1.84 g, 10 mmol) in glacial acetic acid (10 mL) was cooled to 0-5ºC, then hydrochloric acid (10 mL) was added. A solution of sodium nitrite (0.6 g, 10 mmol) in water (5 ml) was then gradually added with stirring. The reaction mixture was left in an ice chest for 15 min. The latter solution of dizonium chloride (**24**) is used in the next coupling reactions directly. To a cold solution of 2-benzoylacetonitrile (**1**) (1.45 g 10 mmol) and sodium acetate trihydrate (3.0 g) in ethanol (50 mL), the diazonium salt **24** was added. The addition was carried out portion-wise with stirring at 0–5°C over a period of 30 min. After complete addition, the reaction mixture was stirred for further 4 h, then kept in an ice-chest for 12 h and finally diluted with water. The product was filtered off, washed with water, dried and recrystallised from EtOH/DMF to give the corresponding hydrazone **25** as buff powder in 80% yield; mp 240-243^{o}C; IR (KBr) ν_{max}/cm^{-1} 3200, 3300 (2NH), 3100 (Aromatic CH), 2225, 2235 (2C≡N), 1650 (C=O), 1560 (C=N); ^{1}H NMR δ 7.55-7.64 (m, 2H, H4 of phenyl of pyrazole and

H4 of ph-CO), 7.65-7.70 (m, 4H, H3, H3` of phenyl of pyrazole, H3 and H3` of phenyl of hydrazone), 7.95-7.97 (m, 2H, H2 and H2` of phenyl of pyrazole), 8.20-8.22 (m, 2H, H2 and H2` of phenyl of hydrazone), 9.61 (s, 1H, NH of hydrazone), 9.91 (s, 1H, NH of pyrazole); ^{13}C NMR δ 78.97 (C4 of pyrazole), 114.08, 127.84 (2C), 128.40, 129.72 (2C), 129.80, 129.89 (2C), 130.95 (2C), 131.73, 132.76, 138.22, 142.38, 151.56, 157.24, 193.44. MS *m/z* (%) 341.23 (M^++1, 2.90), 340.24 (M^+, 12.56), 77.14 (100); Anal. Calcd. For: $C_{19}H_{12}N_6O$ (340.35): C, 67.05; H, 3.55; N, 24.69; Found: C, 67.31; H, 3.73; N, 24.41.

4.2. Biological Evaluation

4.2.1. *In* vitro anti-proliferative activity against Huh-7, HeLa and MCF-7 cell lines

Huh-7 (Hepatocellular Carcinoma) cells, HeLa (cervical adenocarcinoma) cells and MCF-7 (breast adenocarcinoma) cells were used to evaluate the potential cytotoxicity of the tested compounds using the method described by Tim Mosmann [23]. Briefly, in flat bottom 96 well-microplates, cells (0.5×105) were cultured in 180 µl/well RPMI media supplemented with 10% fetal bovine serum, 2µmol/ml L-glutamine, 250 ng/ml fungizone, 100 units/ml penicillin streptomycin solutions at 37°C in a CO_2 incubator. The plates were incubated for 24 h at 37°C in a humidified 5% CO_2 atmosphere to allow cells to settle down. After incubation, cells were then treated with different concentrations of tested compounds or doxorubicin (DOX) as a standard drug (100 – 0.8 µM) and incubated for 24 h at 37 °C, in atmosphere of 5% CO_2. After incubation, the media were removed and MTT solution 40 µl/well was added and incubated for additional 4 h. MTT crystals were solubilized by adding acidified isopropanol (160 µl/well) and the plate was shaken at room temperature. This was followed by photometric determination of the absorbance at 570 nm using the microplate ELISA reader (FLUOstar Omega, BMG, Labtech, Germany). The IC_{50} was determined by using a program Graph-Pad PRISM version 5.

4.2.2. *In* vitro anti-proliferative activity of 11f, 11i and 16b against MDA-MB231 cell lines

MDA-MB231 cells were cultured in Medium Human breast cancer MCF-7 and colon cancer Caco-2 cell lines were maintained in RPMI-1640 supplemented with 100 µg/mL

streptomycin, 100 units/mL penicillin and 10% heat-inactivated fetal bovine serum in a humidified, 5% (v/v) CO_2 atmosphere at 37 ºC.

The tested agent was dissolved in DMSO and kept at a stock concentration of 100 mM. Cell seeding was done at a density of 2000 cells/ well in 96-well plates. Cells were exposed to different treatments for 48 h during which five different drug concentrations were tested. Cytotoxicity was assessed at the end of drug exposure using SRB assay as previously described[27]. Absorbance was measured at 545 nm using microplate reader (BioTek instruments, Vermont, USA). Results were expressed as the relative percentage of absorbance compared to control. Experiments were done in triplicates. Half-maximal inhibitory concentration (IC_{50}), the drug concentration at which 50% growth inhibition is achieved, was calculated using GraphPad Prism software, version 5.00 (GraphPad Software, Inc. La Jolla, CA, USA).

4.2.3. *In* vitro Cell cycle distribution against Huh-7, HeLa and MCF-7 cell lines

After treatment with test compounds for 48 h and paclitaxel (PTX) 1 µM for 24 h as positive control, cells (105 cells) are collected by trypsinization and washed twice with ice-cold PBS (pH 7.4). Cells are re-suspended in two milliliters of 60% ice-cold ethanol and incubated at 4ºC for 1 h for fixation. Fixed cells are washed twice again with PBS (pH 7.4) and resuspended in 1 mL of PBS containing 50 µg/mL RNAase A and 10 µg/mL propidium iodide (PI). After 20 min of incubation in dark at 37 C, cells are analyzed for DNA contents using flow cytometry analysis using FL2 (λex/em 535/617 nm) signal detector (ACEA Novocyte™ flowcytometer, ACEA Biosciences Inc., San Diego, CA, USA). For each sample, 12,000 events are acquired. Cell cycle distribution is calculated using ACEA NovoExpress™ software (ACEA Biosciences Inc., San Diego, CA, USA).

References

[1] M. Chauhan, R. Kumar, Medicinal attributes of pyrazolo[3,4-d]pyrimidines: A review, Bioorg. Med. Chem. 21 (2013) 5657–5668. doi:10.1016/j.bmc.2013.07.027.

[2] A.M. Hussein, Synthesis of some new purine-related compounds: Regioselective one-pot synthesis of new tetrazolo[1,5-a]pyrimidine, pyrazolo[1,5-a]pyrimidine and pyrimido[1,6-a]pyrimidine derivatives, J. Saudi Chem. Soc. 14 (2010) 61–68. doi:10.1016/j.jscs.2009.12.010.

[3] A.K. Ajeesh Kumar, Y.D. Bodke, P.S. Lakra, G. Sambasivam, K.G. Bhat, Design, synthesis and anti-cancer evaluation of a novel series of pyrazolo [1, 5-a] pyrimidine substituted diamide derivatives, Med. Chem. Res. 26 (2017) 714–744. doi:10.1007/s00044-016-1770-0.

[4] T. Novinson, B. Bhooshan, T. Okabe, G.R. Revankar, R.K. Robins, K. Senga, H.R. Wilson, Novel heterocyclic nitrofurfural hydrazones. In vivo antitrypanosomal activity, J. Med. Chem. 19 (1976) 512–516. doi:10.1021/jm00226a013.

[5] Loxo Oncology. Vitrakvi® (Larotrectinib): US prescribing information, (2018). https://www.accessdata.fda.gov/drugsatfda_docs/label/2018/211710s000lbl.pdf.

[6] A. Drilon, R. Nagasubramanian, J.F. Blake, N. Ku, B.B. Tuch, K. Ebata, S. Smith, V. Lauriault, G.R. Kolakowski, B.J. Brandhuber, P.D. Larsen, K.S. Bouhana, S.L. Winski, R. Hamor, W.-I. Wu, A. Parker, T.H. Morales, F.X. Sullivan, W.E. DeWolf, L.A. Wollenberg, P.R. Gordon, D.N. Douglas-Lindsay, M. Scaltriti, R. Benayed, S. Raj, B. Hanusch, A.M. Schram, P. Jonsson, M.F. Berger, J.F. Hechtman, B.S. Taylor, S. Andrews, S.M. Rothenberg, D.M. Hyman, A Next-Generation TRK Kinase Inhibitor Overcomes Acquired Resistance to Prior TRK Kinase Inhibition in Patients with TRK Fusion–Positive Solid Tumors, Cancer Discov. 7 (2017) 963–972. doi:10.1158/2159-8290.CD-17-0507.

[7] T.Z.A. T, A. Geraldine, F. Xavier, J. Cornelius, C.J. Jen, Pyrazolo[1,5- a]pyrimidine derivatives as IRAK4 modulators, 2011.

[8] D. Powell, A. Gopalsamy, Y.D. Wang, N. Zhang, M. Miranda, J.P. McGinnis, S.K. Rabindran, Pyrazolo[1,5-a]pyrimidin-7-yl phenyl amides as novel antiproliferative agents: Exploration of core and headpiece structure–activity relationships, Bioorg. Med. Chem.

Lett. 17 (2007) 1641–1645. doi:10.1016/j.bmcl.2006.12.116.

[9] Y.D. Wang, E. Honores, B. Wu, S. Johnson, D. Powell, M. Miranda, J.P. McGinnis, C. Discafani, S.K. Rabindran, W. Cheng, G. Krishnamurthy, Synthesis, SAR study and biological evaluation of novel pyrazolo[1,5-a]pyrimidin-7-yl phenyl amides as anti-proliferative agents, Bioorg. Med. Chem. 17 (2009) 2091–2100. doi:10.1016/j.bmc.2008.12.046.

[10] A. Kamal, J.R. Tamboli, V.L. Nayak, S.F. Adil, M.V.P.S. Vishnuvardhan, S. Ramakrishna, Synthesis of pyrazolo[1,5-a]pyrimidine linked aminobenzothiazole conjugates as potential anticancer agents, Bioorg. Med. Chem. Lett. 23 (2013) 3208–3215. doi:10.1016/j.bmcl.2013.03.129.

[11] J. Li, Y.F. Zhao, X.L. Zhao, X.Y. Yuan, P. Gong, Synthesis and Anti-tumor Activities of Novel Pyrazolo[1,5-a]pyrimidines, Arch. Pharm. (Weinheim). 339 (2006) 593–597. doi:10.1002/ardp.200600098.

[12] M.M. El-Enany, M.M. Kamel, O.M. Khalil, H.B. El-Nassan, Synthesis and antitumor activity of novel pyrazolo[1,5-a]pyrimidine derivatives, Eur. J. Chem. 2 (2011) 331–336. doi:10.5155/eurjchem.2.3.331-336.319.

[13] N. Gommermann, P. Buehlmayer, A. von Matt, W. Breitenstein, K. Masuya, B. Pirard, P. Furet, S.W. Cowan-Jacob, G. Weckbecker, New pyrazolo[1,5a]pyrimidines as orally active inhibitors of Lck, Bioorg. Med. Chem. Lett. 20 (2010) 3628–3631. doi:10.1016/j.bmcl.2010.04.112.

[14] M.P. Dwyer, K. Paruch, M. Labroli, C. Alvarez, K.K.M. Keertikar, C. Poker, R. Rossman, T.O. Fischmann, J.S. Duca, V. Madison, D. Parry, N. Davis, W. Seghezzi, D. Wiswell, T.J. Guzi, K. Paruch, M.P. Dwyer, C. Alvarez, K.K.M. Keertikar, C. Poker, R. Rossman, J.S. Duca, T.O. Fischmann, V. Madison, D. Parry, N. Davis, W. Seghezzi, D. Wiswell, T.J. Guzi, Discovery of pyrazolo[1,5-a]pyrimidine-based CHK1 inhibitors: A template-based approach—Part 2, Bioorg. Med. Chem. Lett. 21 (2011) 471–474. doi:10.1016/j.bmcl.2010.10.114.

[15] O.M. Ahmed, M.A. Mohamed, R.R. Ahmed, S.A. Ahmed, Synthesis and anti-tumor activities of some new pyridines and pyrazolo[1,5-a]pyrimidines, Eur. J. Med. Chem. 44 (2009) 3519–3523. doi:10.1016/j.ejmech.2009.03.042.

[16] Y. Tominaga, Y. Matsuoka, S. Kohra, A. Hosomi, A Novel Preparation of Polarized

Ethylenes by the Reaction of Thioamides or Dithiocarboxylates with Tetracyanoethylene Oxide. Synthesis of Pyrazoles and Pyrimides, Heterocycles. 26 (1987) 613. doi:10.3987/R-1987-03-0613.

[17] P.L. Southwick, B. Dhawan, Preparation of 4,6-diaminopyrazolo[3,4- d] pyrimidines with variations in substitution at the 1- and 3-positions, J. Heterocycl. Chem. 12 (1975) 1199–1205. doi:10.1002/jhet.5570120621.

[18] I.C. Christoforou, P.A. Koutentis, New regiospecific isothiazole C–C coupling chemistry, Org. Biomol. Chem. 4 (2006) 3681–3693. doi:10.1039/B607442A.

[19] S. Kantevari, M.V. Chary, S.V.N. Vuppalapati, A highly efficient regioselective one-pot synthesis of 2,3,6-trisubstituted pyridines and 2,7,7-trisubstituted tetrahydroquinolin-5-ones using K5CoW12O40·3H2O as a heterogeneous recyclable catalyst, Tetrahedron. 63 (2007) 13024–13031. doi:10.1016/j.tet.2007.10.014.

[20] S.K. Prajapti, A. Nagarsenkar, S.D. Guggilapu, K.K. Gupta, L. Allakonda, M.K. Jeengar, V.G.M. Naidu, B.N. Babu, Synthesis and biological evaluation of oxindole linked indolyl-pyrimidine derivatives as potential cytotoxic agents, Bioorg. Med. Chem. Lett. 26 (2016) 3024–3028. doi:10.1016/j.bmcl.2016.05.019.

[21] G. Dou, P. Xu, Q. Li, Y. Xi, Z. Huang, D. Shi, Clean and Efficient Synthesis of Isoxazole Derivatives in Aqueous Media, Molecules. 18 (2013) 13645–13653. doi:10.3390/molecules181113645.

[22] Y. Zhou, Y. Dun, H. Fu, L. Wang, X. Pan, X. Yang, H. Fang, Design, synthesis, and preliminary bioactivity evaluation of N -benzylpyrimidin-2-amine derivatives as novel histone deacetylase inhibitor, Chem. Biol. Drug Des. 90 (2017) 936–942. doi:10.1111/cbdd.13019.

[23] T. Mosmann, Rapid colorimetric assay for cellular growth and survival: Application to proliferation and cytotoxicity assays, J. Immunol. Methods. 65 (1983) 55–63. doi:10.1016/0022-1759(83)90303-4.

[24] P. Banerjee, A.O. Eckert, A.K. Schrey, R. Preissner, ProTox-II: a webserver for the prediction of toxicity of chemicals, Nucleic Acids Res. 46 (2018) W257–W263. doi:10.1093/nar/gky318.

[25] F. Al-Qalaf, F. Mandani, M.M. Abdelkhalik, A.A. Bassam, Synthesis of 5-Substituted 3-Amino-1H-Pyrazole-4-Carbonitriles as Precursors for Microwave Assisted Regiospecific

Syntheses of Pyrazolo[1,5-a]Pyrimidines, Molecules. 14 (2008) 78–88. doi:10.3390/molecules14010078.

[26] D.E. Tupper, M.R. Bray, Steric and Electronic Control in the Addition of Hydrazine and Phenylhydrazine to α-[(Dimethylamino)methylene]-β-oxoarylpropanenitriles, Synthesis (Stuttg). 1997 (1997) 337–341. doi:10.1055/s-1997-1186.

[27] M.F. Tolba, S.Z. Abdel-Rahman, Pterostilbine, an active component of blueberries, sensitizes colon cancer cells to 5-fluorouracil cytotoxicity, Sci. Rep. 5 (2015) 15239. https://doi.org/10.1038/srep15239.

Graphical Abstract

Synthesis and *in-vitro* anti-proliferative evaluation of some pyrazolo[1,5-*a*]pyrimidines as novel larotrectinib analogs

Mohamed H. Attia[1], Eman Z. Elrazaz[2], Soad Z. El-Emam[3], Azza T. Taher[4], Hatem A. Abdel-Aziz[5*] and Khaled A.M. Abouzid[2,6*]

Pyrazolopyrimidines **11f**, **16b** and **11i** showed potent antiproliferative activity towards Huh-7, HeLa and MCF-7 cell lines with IC_{50} = 6.3, 7.8 and 3.0 µM, whereas **11i** and **16b** exhibited IC_{50} = 4.32 µM and 5.74 µM, against MDA-MB231 cell lines. **11i** induced a reduction in G1 phase with arrest in S phase and G2/M phase of MCF-7 cells. **16b** induced a reduction in G1 phase and arrest in G2/M phase of Hela cells. **11i** induced arrest in G1 phase and reduction in S phase of MDA-MB-231 cells.

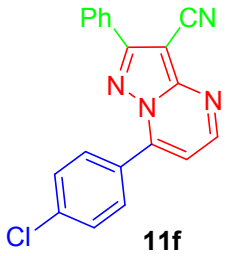

11f

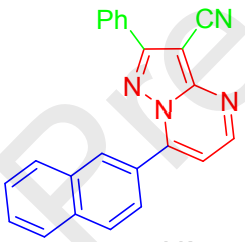

11i

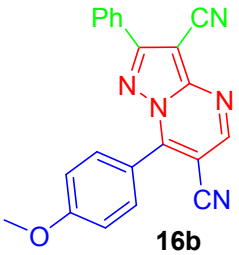

16b

Highlights

- A series of pyrazolo[1,5-*a*]pyrimidines **11a-j**, **16a-c** and **22** were synthesized.
- The anticancer activity against 4 human cancer cell lines was evaluated.
- **11f**, **16b** and **11i** emerged as the most active compounds against 4 tested cells.
- **11i** and **16b** showed potent activity against MDA-MB231 cell lines.
- **11i** induced a reduction in G1 phase with arrest in S and G2/M phase of MCF-7 cells.
- **16b** induced a reduction in G1 phase with arrest in G2/M phase of Hela cells.
- **11i** induced an arrest in G1 phase with reduction in S phase of MDA-MB-231.

There are no interests to declare